

HAVE WE DETECTED PATCHY REIONIZATION IN QUASAR SPECTRA?

ADAM LIDZ¹, S. PENG OH², AND STEVEN R. FURLANETTO³

¹ Harvard-Smithsonian Center for Astrophysics, 60 Garden Street, Cambridge, MA 02138, USA

² Department of Physics, University of California, Santa Barbara, CA 93106

³ Division of Physics, Mathematics, & Astronomy, California Institute of Technology, Mail Code 130-33, Pasadena, CA 91125

Electronic mail : alidz@cfa.harvard.edu, peng@physics.ucsb.edu, sfurlane@tapir.caltech.edu

July 18, 2018. To be submitted to ApJ.

ABSTRACT

The Ly α forest at $z \gtrsim 5.5$ shows strong scatter in the mean transmission even when smoothed over very large spatial scales, $\gtrsim 50$ Mpc/ h . This has been interpreted as a signature of strongly fluctuating radiation fields, or patchy reionization. To test this claim, we calculate the scatter arising solely from density fluctuations, with a uniform ionizing background, using analytic arguments and simulations. This scatter alone is comparable to that observed. It rises steeply with redshift and is of order unity by $z \sim 6$, even on ~ 50 Mpc/ h scales. This arises because: i) at $z \sim 6$, transmission spectra, which are sensitive mainly to rare voids, are highly biased (with a linear bias factor $b \geq 4 - 5$) tracers of underlying density fluctuations, and ii) projected power from small-scale transverse modes is aliased to long wavelength line-of-sight modes. Inferring patchy reionization from quasar spectra is therefore subtle and requires much more detailed modeling. Similarly, we expect order unity transmission fluctuations in the $z \sim 3$ HeII Ly α forest from density fluctuations alone, on the scales over which these measurements are typically made.

Subject headings: cosmology: theory – intergalactic medium – large scale structure of universe; quasars – absorption lines

1. INTRODUCTION

At redshifts close to $z \sim 3$, the structure in the Ly α forest has been shown to arise naturally from density fluctuations in the cosmic web (e.g. Miralda-Escudé et al. 1996). At sufficiently high redshift, however, the structure in the Ly α forest may instead largely reflect the topology of reionization, and/or a strongly fluctuating radiation field. In high-redshift quasar spectra with extended opaque regions, significant gaps of substantial transmission occur (e.g. Becker et al. 2001, White et al. 2003, White et al. 2005). This has previously been attributed to a strongly fluctuating UV background, as expected at the tail end of reionization (Wyithe & Loeb 2005, Fan et al 2005).

Could these transmission gaps simply arise from underdense regions where the neutral hydrogen fraction is lower? The transmission in the $z \sim 6$ quasar spectra differs significantly from sightline to sightline, even when one averages over co-moving length scales of $\sim 50 - 100$ Mpc/ h . Since the density variance is small over such large scales, one might naively expect that the reionization of the IGM must be incomplete near $z \sim 6$.

In this *Letter*, we critically examine this naive intuition. Is rapidly increasing scatter in sightline to sightline flux transmission a good diagnostic for patchy reionization (Fan et al. 2002, Lidz et al. 2002, Sokasian et al. 2003, Paschos & Norman 2005)? We find that in fact the fractional scatter in the mean transmissivity of the IGM will be large at high redshift, even for a completely uniform ionizing background. An analogous calculation applies to the case of the HeII Ly α forest near $z \sim 3$.

2. THE FLUX POWER SPECTRUM

We adopt the usual ‘gravitational instability’ model of the Ly α forest valid at $z \sim 3$ (e.g., Hui et al 1997).

In particular, we assume an isothermal gas and a uniform radiation field, to see if these assumptions demonstrably break down at $z \sim 6$. Assuming photoionization equilibrium, the Ly α optical depth is $\tau = A\Delta^2$, where $A \propto (1+z)^{4.5}T^{-0.7}/\Gamma$, and the transmitted flux is $F = e^{-\tau}$. We study the fluctuations in transmitted flux, $\delta_F = (F - \langle F \rangle)/\langle F \rangle$, and the line of sight power spectrum of these fluctuations, $P_F(k)$. We will also refer to the effective optical depth, $\tau_{\text{eff}} = -\ln\langle F \rangle$.

It is important to note that $P_F(k)$ is related to the underlying power spectrum of density fluctuations $P_\delta(k)$ in a rather complicated way. First, gas pressure smooths the baryon-density distribution on small scales with respect to the dark matter. Second, a non-linear transformation maps density into optical depth ($\tau \propto \Delta^2$). Third, one maps from real space to skewers in redshift space, projecting from 3D to 1D and incorporating the effect of peculiar velocities. Fourth, one convolves the optical depth distribution with the thermal broadening kernel. Finally, a second non-linear transformation maps τ into transmitted flux ($F = e^{-\tau}$). These issues are well studied in the context of the $z \sim 3$ Ly α forest (e.g. Croft et al. 2002) but are under-appreciated in the reionization literature. Previous neglect of this physics has led to erroneous conclusions.

2.1. Analytic Estimates

We will therefore require numerical simulations to model the flux power spectrum in detail, and its dependence on redshift and the mean transmissivity of the IGM. We can nonetheless anticipate the results with analytic arguments. Specifically, we estimate the point-to-point flux variance as a function of A and τ_{eff} . We perform this calculation using the Miralda-Escudé et al.

(2001) fitting formula for the gas density PDF:

$$P(\Delta)d\Delta = G\Delta^{-b}\exp\left[-\frac{(\Delta^{-2/3} - C)^2}{8\delta_0^2/9}\right]d\Delta. \quad (1)$$

Here the parameters G and C are fixed by requiring the PDF to normalize to unity and to satisfy $\langle\Delta\rangle = 1$. The other parameters are given by $\delta_0 = 7.61/(1+z)$ and $b = 2.5$ at $z = 6$. We then calculate the first two moments of the (unsmoothed) flux distribution, $\langle F \rangle = \langle e^{-A\Delta^2} \rangle$, and $\langle F^2 \rangle = \langle e^{-2A\Delta^2} \rangle$, by integrating over the gas density PDF. These estimates ignore the effect of peculiar velocities and thermal broadening, but we include these effects subsequently using our simulations.

These integrals can be approximated using the method of steepest descents (Songaila & Cowie 2002), to give $\langle F \rangle \sim c\tilde{A}^{1/4}\exp[-d\tilde{A}^{0.4}]$, and $\langle F^2 \rangle/\langle F \rangle^2 \sim \tilde{c}\tilde{A}^{-1/4}\exp[\tilde{d}\tilde{A}^{0.4}]$, where c , d , \tilde{c} , and \tilde{d} are constants, and $\tilde{A} = A/25$. We find that $c = 5.3$, $d = 5.1$, $\tilde{c} = 0.22$, and $\tilde{d} = 3.5$ provide a good approximation to the results of full numerical integrations. These scalings immediately suggest that the fractional point-to-point dispersion will be quite large when A and τ_{eff} are also large, *even assuming a homogeneous radiation field*. For instance, when $\tau_{\text{eff}} \sim 5$, we expect the fractional point-to-point dispersion to be $\sigma_F/\langle F \rangle \sim 4$. On the other hand, when $\tau_{\text{eff}} \sim 1$, the point-to-point dispersion is only $\sigma_F/\langle F \rangle \sim 0.8$. When the transmission becomes small, it is dominated by rare voids, which drastically increases the point-to-point variance.

2.2. Numerical Calculations

In order to make a more accurate calculation, and to consider transmission fluctuations smoothed over large scales, we calculate the flux power spectrum numerically. We use a Hydro-Particle-Mesh (HPM) (Gnedin & Hui 1998) simulation with 2×512^3 particles and 512^3 mesh-points in a $40 h^{-1}$ Mpc box, assuming a Λ CDM cosmology with $(\sigma_8, h, \Omega_b h^2, \Omega_m, \Omega_\Lambda) = (0.84, 0.7, 0.02, 0.3, 0.7)$. The simulation is an implementation of HPM into the parallel N-body code, Mc² (see Heitmann et al. 2005 for detailed tests of Mc², and the Appendix of Lidz et al. 2005, Habib et al. 2006, in prep., for the details and convergence studies of our implementation of HPM).

We take the baryon density and peculiar velocity fields from the simulation and extract artificial spectra in the usual manner (for more details see e.g., Hui, Gnedin & Zhang 1997). Specifically, we consider $z = 4.9, 5.3, 5.7, 6.0$, and adjust A to match $\langle F \rangle = 0.20, 0.13, 0.06$, and 0.01. These values are close to, but slightly larger than, the observational measurements of Becker et al. (2001), White et al. (2003), and Fan et al. (2005). For each redshift, we extract 5,000 artificial spectra from the simulation box.

In order to consider large-scale transmission fluctuations, we need to extrapolate to scales beyond the size of the simulation box. We do so assuming that on large scales, the flux power spectrum and the 1D linear matter power spectrum differ only in normalization and not in shape (linear biasing, e.g., Scherrer & Weinberg 1998, Lidz et al. 2002), although we will show in §3 that the bias *increases sharply with increasing redshift*. We

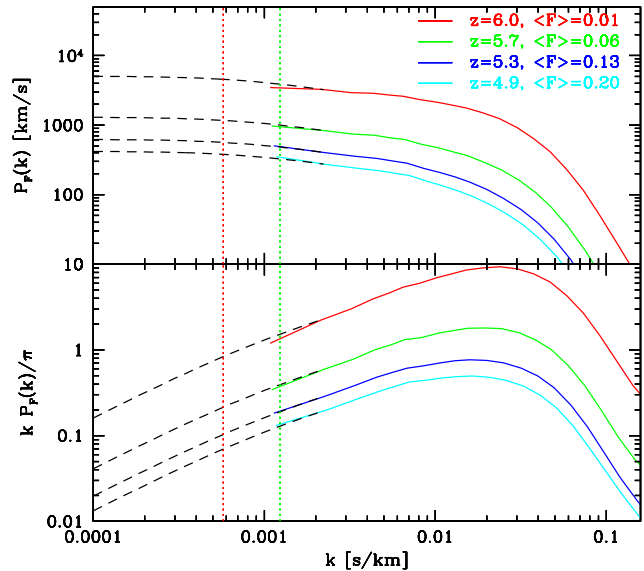


FIG. 1.— Flux power spectrum as a function of scale at various redshifts, with A adjusted to the mean flux level $\langle F \rangle$ shown. The black dashed lines show the large-scale extrapolations of the simulation results described in the text. The green and red dotted lines correspond to the length scales $L = 35, 75$ Mpc/h at $z = 6$ respectively. Notice that $kP_F(k)$ decreases only slowly towards large scales, a consequence of aliasing, as we describe in the text. At $z \sim 6$, the fluctuations are of order unity even on scales close to ~ 50 Mpc/h.

normalize the extrapolation to the simulated flux power spectrum at $k \sim k_f/2$, where k_f is the wavenumber associated with the fundamental mode of the box. We generally consider smoothing scales only somewhat larger than the size of our simulation box, $L_{\text{box}} = 40$ Mpc/h. Furthermore, the flux power spectrum is relatively flat on these scales, and so our results are not terribly sensitive to the details of this extrapolation.¹

In Fig 1, we show the flux power spectrum from our simulations. The amplitude of transmission fluctuations clearly increases rapidly with redshift, despite declining density fluctuations. In fact, fractional fluctuations are of order unity on scales of $L \sim 35$ Mpc/h at $z \sim 6$, *even for a uniform radiation field*. This implies that it may be difficult to discern patchy reionization from transmission fluctuations. We study this further in §3.

Another interesting feature of Fig 1 is that the flux power spectrum is quite flat: $kP_F(k)$ declines only gradually towards large scales. This is because absorption spectra provide only a 1D skewer through the IGM, with a power spectrum (ignoring redshift space distortions for illustrative purposes):

$$P_{1d}(k_{\parallel}) = \int_{k_{\parallel}}^{\infty} \frac{dk}{2\pi} k P_{3d}(k). \quad (2)$$

¹ For instance, if we extrapolate our results using a power law, our estimate of the transmission dispersion, Eq. (3), changes by $\sim 20\%$.

Thus, the 1D power spectrum falls off much more slowly towards large scales than the 3D power spectrum. This is the well-known process of aliasing found in pencil-beam galaxy surveys (Kaiser & Peacock 1991), whereby short transverse wavelength modes in projection alias power to long wavelength, line of sight modes. To illustrate this quantitatively, we consider the amplitude of 3D fluctuations in the non-linear baryon-density field, $\Delta_b^2(k) = k^3 P_b(k)/(2\pi^2)$, approximating the relation between the baryonic and dark matter power spectra as $P_b(k) = e^{-2k^2/k_f^2} P_{\text{dm}}(k)$, assuming $k_f = 20h \text{ Mpc}^{-1}$ (Gnedin & Hui 1998), and using fitting formulae from Peacock & Dodds (1996) and Eisenstein & Hu (1999). We contrast this with the variance of 1D baryonic fluctuations, $\Delta_{\text{1D,b}}^2(k_{\parallel}) = k_{\parallel} P_{\text{1D,b}}(k_{\parallel})/\pi$, comparing line of sight fluctuations of wavenumber k_{\parallel} to 3D fluctuations with wavenumber $|\vec{k}| = k_{\parallel}$. The 1D power spectrum is a factor of ~ 5.5 – 10.6 times larger than the 3D power spectrum for modes with wavelength $L \sim 50$ – $100 \text{ Mpc}/h$. Fluctuations averaged over a skewer of a given length are much larger than fluctuations averaged over an entire sphere of comparable size.

3. THE SIGHTLINE TO SIGHTLINE SCATTER

Given $P_F(k)$, the fractional sightline-to-sightline variance in the transmission is (Lidz et al. 2002):

$$\frac{\sigma_{\langle F \rangle}^2}{\langle F \rangle^2} = 2 \int_0^{\infty} \frac{dk}{2\pi} P_F(k) \left[\frac{\sin(kL/2)}{(kL/2)} \right]^2. \quad (3)$$

Shot-noise is negligible for significant stretches of spectrum with at least moderate signal to noise (see Lidz et al. 2002 for details). We consider the fractional dispersion in the mean transmitted flux, $\sigma_{\langle F \rangle}/\langle F \rangle$, as opposed to the absolute dispersion, $\sigma_{\langle F \rangle}$. Note that $\sigma_{\tau_{\text{eff}}} = \sigma_{\langle F \rangle}/\langle F \rangle$ for small fluctuations.

We show this quantity in Fig. 2. As in the flux power spectrum calculation (Fig. 1), the fractional dispersion increases rapidly with decreasing transmission, and falls off only slowly as the smoothing scale becomes large². By $z \sim 6$, assuming $\langle F \rangle = 0.01$ ($\tau_{\text{eff}} = 4.6$), a complete absorption trough $\langle F \rangle = 0$ of length $\sim 50 \text{ Mpc}/h$ is only a $\sim 1 - \sigma$ fluctuation, even though density fluctuations are small, $\sigma_{\rho,1D} \sim 0.2$ on these scales. Transmission fluctuations are a highly biased tracer of underlying density fluctuations at high redshift, with a bias factor of $b = (\sigma_{\langle F \rangle}/\langle F \rangle)/\sigma_{\rho,1D} \sim 4$ when $\tau_{\text{eff}} \sim 4 - 5$ (and increasing at higher τ_{eff}). Although on large scales the flux and density power spectra have the same shape, one can *not* then simply assume that $\sigma_{\langle F \rangle}/\langle F \rangle \sim \sigma_{\rho,1D}$, as has previously been done (Wyithe & Loeb 2005, Fan et al. 2005).

Note that state of the art reionization simulations have thus far been done with boxsizes of less than $10 \text{ Mpc}/h$ (e.g. Gnedin 2000, Sokasian et al. 2003, Paschos & Norman 2005), although steps towards large scale simulations are being made (Kohler et al. 2005, Iliev et al. 2005). It is common practice to generate mock spectra from these simulations by wrapping long lines of sight around these small periodic boxes many times. From Fig.

² Since, on large scales, the flat $P_F(k)$ is close to a white noise power spectrum, $\sigma_{\langle F \rangle}^2/\langle F \rangle^2 \propto L^{-1}$.

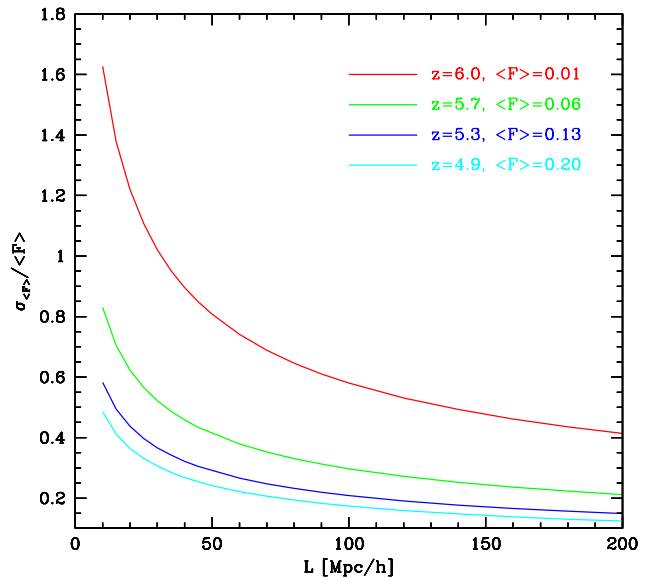


FIG. 2.— Sightline-to-sightline scatter in the mean transmission as a function of scale and redshift. The cyan, blue, green, and red curves indicate the expected scatter in the mean transmission as a function of scale at redshifts $z = 4.9, 5.3, 5.7$ and 6 respectively. The fractional scatter increases rapidly with decreasing transmission, and dies off only slowly towards large scales.

1 and Eq. 3, it is clear that estimates of the transmissivity scatter from mock spectra generated in this way are *underestimates*. For instance, the best case scenario for extrapolating Paschos & Norman (2005) to larger scales would have a flat line of sight power spectrum on scales larger than their box ($L_{\text{box}} = 6.8 \text{ Mpc}/h$) and match our results on smaller scales. Even in this best case, we calculate that they underestimate the transmissivity variance by a factor of ~ 2 for a smoothing scale of $L = 50 \text{ Mpc}/h$.

Equation (3) does not capture the full story since the flux probability distribution is non-Gaussian. This is obvious since fluctuations in the mean transmission are of order unity, yet the transmission is bounded between zero and one. To reliably calculate confidence intervals, we thus need to consider the full shape of the PDF of the transmission, smoothed on large scales. Because the extrapolation of the full PDF to large scales is non-trivial (unlike for the simple power spectrum), we will calculate the PDF directly from the simulation box. Thus we effectively smooth on scales of $L = L_{\text{box}} = 40 \text{ Mpc}/h$ but underestimate the width of the PDF because of large-scale power missing from our box. We show the PDF of τ_{eff} in the bottom panel of Fig. 3. It becomes increasingly broad and skewed, with a long tail towards high optical depth at high redshift. This asymmetry implies a bias in measurements of τ_{eff} from samples with a small number of sightlines.

The top panel of Fig. 3 shows error bands for the expected sightline to sightline scatter in the effective optical depth as a function of redshift, adopting a smoothing length of $L = 40 \text{ Mpc}/h$. Even for large smoothing

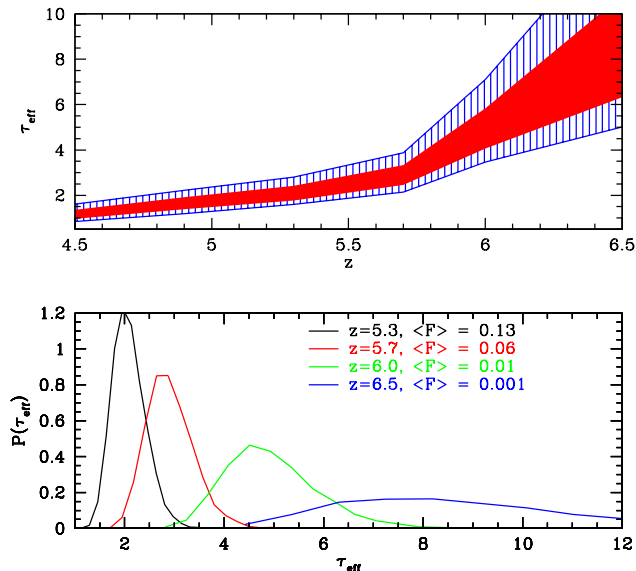


FIG. 3.— Evolution of τ_{eff} and the expected sightline to sightline scatter. The top panel shows 68% and 95% confidence regions for the effective optical depth, given a smoothing length of $L = 40 \text{ Mpc}/h$. Notice that the shaded regions become quite broad at large τ_{eff} . We assume central τ_{eff} values of $\langle F \rangle = 0.32, 0.20, 0.13, 0.06, 0.01$, at $z = 4.5, 4.9, 5.3, 5.7, 6.0$, and 6.5 respectively. The upper limits on τ_{eff} at $z = 6.5$ extend beyond the edge of the plot. They are $\tau_{\text{eff}} = 10.8, 14$ at 68% and 95% confidence, respectively. The bottom panel shows examples of the corresponding PDFs.

scales, the scatter increases rapidly with redshift. We therefore caution against over-interpreting the increasing scatter seen in plots of $\tau_{\text{eff}}(z)$ seen in the literature

How does the level of scatter we predict compare with existing observations? We compare with recent measurements from Fan et al. (2005) (their Table 5), which indicate a dispersion of $\tau = (2.1 \pm 0.3, 2.5 \pm 0.5, 2.6 \pm 0.6, 3.2 \pm 0.8, 4.0 \pm 0.8, 7.1 \pm 2.1)$ at $z = (4.90 - 5.15, 5.15 - 5.35, 5.35 - 5.55, 5.55 - 5.75, 5.75 - 5.95, 5.95 - 6.25)$. The values of the dispersion in the last two-redshift bins are lower limits, since some lines of sight in these bins show complete absorption troughs. Interpolating from our results, which assume a different redshift evolution for τ_{eff} , we find $\tau = (2.1^{+0.38}_{-0.28} {}^{+0.79}_{-0.47}, 2.5^{+0.46}_{-0.32} {}^{+0.94}_{-0.58}, 2.6^{+0.48}_{-0.33} {}^{+0.98}_{-0.61}, 3.2^{+0.67}_{-0.39} {}^{+1.4}_{-0.78}, 4.0^{+0.99}_{-0.48} {}^{+2.0}_{-0.98}, 7.1^{+3.9}_{-0.60} {}^{+7.1}_{-1.9})$, where the intervals indicate 68% and 95% confidence regions. Note that Fan et al. (2005) considered a smoothing scale of $\Delta z = 0.15$, corresponding to $L = 44$ (56) Mpc/h at $z = 6$ (5). Our numbers assume a slightly different scale, $L = 40 \text{ Mpc}/h$, throughout, due to the limited size of our simulation box. From this comparison, we conclude that our results are broadly consistent with the measurements of Fan et al. (2005), although we remark that the dispersion is not the ideal statistic to compare with since the PDF of τ_{eff} is asymmetric. We reiterate that *our calculations assume a uniform radiation field and indicate a scatter that is already comparable to the measured values.*

Furthermore, there are several systematic effects, each

of which likely tends to *increase* the observed scatter in the mean transmissivity relative to our predictions. First, as remarked previously, our simulations have a limited boxsize ($L = 40 \text{ Mpc}/h$) and therefore miss large scale power. Second, at high redshift the quasar continuum is generally estimated using a single power-law, extrapolating from redward of the Ly α forest (e.g. Fan et al. 2005). In reality, the quasar continuum has structure and varies significantly from quasar to quasar (e.g. Bernardi et al. 2003). As a result, some of the apparent transmissivity fluctuations in the data may actually be due to fluctuations in the quasar continuum. Next, Lyman limit systems are under-produced in simulations, yet they add large scale power to the transmission (e.g. McDonald et al. 2005), which may lead us to underestimate the transmissivity scatter. Finally, metal-line absorbers are inevitably present in the observed Ly α forest yet are not included in our calculations. We refer the reader to Tytler et al. (2004) for further quantitative discussion of these systematics at $z \sim 2 - 3$.

3.1. Sightline-to-Sightline Scatter in the Ly β forest

How about the transmissivity scatter in the Ly β forest? We can estimate the fluctuations in the $z \sim 6$ transmissivity of the Ly β region of a quasar spectrum using Eq. 3, but we must consider fluctuations in the foreground Ly α forest as well. Dijkstra et al. (2004) show that the total power spectrum $P_{F,\text{tot}}$ is:

$$P_{F,\text{tot}}(k) = P_{F,\alpha}(k) + P_{F,\beta}(k) + \int \frac{dk'}{2\pi} P_{F,\alpha}(k - k') P_{F,\beta}(k'). \quad (4)$$

This equation reflects the fact that foreground gas, absorbing in Ly α , is widely separated in physical space, and hence independent of, gas absorbing in Ly β . The last term in Eq. 4 occurs because the total correlation function then involves a product, which transforms into a convolution term. Although higher-order in the transmissivity fluctuations (Dijkstra et al. 2004), this term cannot be ignored here because the fluctuations are so large (it increases the total variance by $\sim 10 - 20\%$).

Nonetheless, over an equivalent comoving patch, transmission fluctuations in the Ly β forest are substantially smaller than in the Ly α forest. We can see this heuristically from §2.1: $\langle F^2 \rangle / \langle F \rangle^2 \sim \tilde{c} \tilde{A}^{-1/4} \exp[\tilde{d} \tilde{A}^{0.4}]$, and $\tilde{A}_\beta = \tilde{A}_\alpha / 6.24$. In practice, this works out to fractional fluctuations which are $\sim 2 - 4$ times smaller in the Ly β forest. From the simulations, over a $50 \text{ Mpc } h^{-1}$ interval, if we assume $\langle F_\alpha \rangle = (0.2, 0.01)$, at $z = (4.9, 6)$ (and thus $\langle F_\beta \rangle [z = 6] = 0.19$ – see Oh & Furlanetto 2005 for details on the relation between the Ly α and Ly β absorption in a clumpy IGM), we obtain $\sigma_{(F_{\text{tot}})} / \langle F_{\text{tot}} \rangle \sim 0.35$, compared to $\sigma_{(F)} / \langle F \rangle = 0.8$ for Ly α fluctuations. If instead $\langle F_\alpha \rangle = 0.001$ at $z = 6$ (and thus $\langle F_\beta \rangle [z = 6] = 0.085$), we obtain $\sigma_{(F_{\text{tot}})} / \langle F_{\text{tot}} \rangle \sim 0.45$, compared to $\sigma_{(F)} / \langle F \rangle \sim 2$ for Ly α fluctuations. Thus, in principle the Ly β forest is a much more robust indicator of a fluctuating radiation field. Unfortunately, due to contamination from the Ly γ forest, at present the Ly β forest suffers from small-number statistics. For instance, Fan et al. (2005) have 97 vs. 19 measurements of the Ly α and Ly β forests respectively, of size $\Delta z = 0.15$, spanning $z = 4.8 - 6.3$ in Ly α , and $z = 5.3 - 6.3$ in Ly β . The observed scatter in

the Ly β forest (their Fig. 3) is consistent with density fluctuations alone.

3.2. Sightline-to-Sightline Scatter in the HeII Forest

Finally, we point out that a very similar calculation applies to the sightline-to-sightline scatter in the transmissivity of the HeII Ly α forest near $z \sim 3$. Specifically, we measure the flux power spectrum in the HeII Ly α forest using a lower redshift simulation output, adopting $\tau_{\text{eff,HeII}} \sim 4$ at $z = 2.9$ based on the measurements of Smette et al. (2002). These measurements are performed in narrow bins with co-moving length scales of $L \sim 18\text{--}36$ Mpc/ h . At $z = 2.9$, we find that the rms fractional fluctuation in the HeII Ly α transmissivity on these smoothing scales is $\sigma_{\langle F_{\text{HeII}} \rangle} / \langle F_{\text{HeII}} \rangle = 1.6 - 1.2$. Again, we caution against interpreting the observed scatter as a signature of fluctuations in the HeII ionizing background.

4. CONCLUSIONS

We do not mean to imply that the radiation field is indeed uniform at $z \sim 6$. Our intent is only to show that ruling out the *null hypothesis* that the scatter in

the high redshift Ly α forest results solely from density fluctuations is subtle. Indeed, we find that transmissivity fluctuations should be *of order unity* at $z \sim 6$ on scales of $L \sim 50$ Mpc/ h , from density fluctuations alone. We therefore caution against over-interpreting the large scatter in τ_{eff} seen in the spectra of $z \sim 6$ quasars or the analogous scatter seen in the $z \sim 3$ HeII Ly α forest. In future work, we intend to model the effect of inhomogeneous reionization on the statistics of the Ly α forest, following up on the work of Furlanetto & Oh (2005), and to design statistical measures to discern the presence or absence of these fluctuations.

ACKNOWLEDGMENTS

AL thanks Katrin Heitmann and Salman Habib for their collaboration in producing the HPM simulation used in this analysis. We thank Matias Zaldarriaga for useful discussions and comments on a draft. We thank Lars Hernquist, Lam Hui and Oliver Zahn for stimulating conversations. SPO acknowledges NSF grant AST0407084 for support.

REFERENCES

- Becker, R. H. et al. 2001, AR, 122, 2850
 Bernardi, M., et al. 2003, AJ, 125, 32
 Cen, R. & McDonald, P. 2002, ApJ, 570, 457
 Croft, R. A. C., Weinberg, D. H., Bolte, M., Burles, S., Hernquist, L., Katz, N., Kirkman, D. & Tytler, D. 2002, ApJ, 581, 20
 Dijkstra, M., Lidz, A., & Hui, L. 2004, ApJ, 605, 7
 Eisenstein, D. J., & Hu, W. 1999, ApJ, 511, 5
 Fan, X. et al. 2002, AJ, 123, 1247
 Fan, X. et al. 2005, AJ submitted, astro-ph/0512082
 Furlanetto, S. R., & Oh, S. P. 2005, MNRAS, 363, 1031
 Gnedin, N. Y., & Hui, L. 1998, MNRAS, 296, 44
 Gnedin, N. Y., 2000, ApJ, 535, 530
 Heitmann, K., Ricker, P. M., Warren, M. S., & Habib, S. 2005, ApJS, 160, 28
 Hui, L., Gnedin, N. Y., & Zhang, Y., 1997, ApJ 486, 599
 Iliiev, I. T., Mellema, G., Pen, U., Merz, H., Shapiro, P. R., & Alvarez, M. A. 2002, MNRAS, submitted, astro-ph/0512187
 Kaiser, N., & Peacock, J. A. 1991, ApJ, 379, 482
 Kohler, K., Gnedin, N. Y., & Hamilton, A. J. S. 2005, astro-ph/0511627
 Lidz, A., Hui, L., Zaldarriaga, M., & Scoccimarro, R. 2002, ApJ, 579, 491
 Lidz, A., Heitmann, K., Hui, L., Rauch, M., & Sargent, W. L. W. 2005, ApJ, in press, astro-ph/0505138
 McDonald, P. et al. 2000, ApJ, 543, 1
 McDonald, P. et al. 2005, MNRAS, 360, 1471
 Miralda-Escudé, J., Cen, R., Ostriker, J. P., Rauch, M., 1996, ApJ, 471, 582
 Miralda-Escudé, J., Haehnelt, M. G., & Rees, M. J. 2000, ApJ, 530, 1
 Oh, S. P., & Furlanetto, S. R. 2005, ApJL, 620, 9
 Paschos, P., & Norman, M. L. 2005, ApJ, 631, 59
 Peacock, J. A., & Dodds, S. J. 1996, MNRAS, 280L, 19
 Scherrer, R. J., & Weinberg, D. H. 1998, ApJ, 504, 607
 Smette, A. et al. 2002, ApJ, 564, 542
 Sokasian, A., Abel, T., & Hernquist, L. 2003, MNRAS, 340, 473
 Songaila, A., & Cowie, L. 2002, AJ, 123, 2183
 Tytler, D. et al. 2004, ApJ, 617, 1
 White, R. L., Becker, R. H., Fan, X., & Strauss, M. A. 2003, AJ, 126, 1
 White, R. L., Becker, R. H., Fan, X., & Strauss, M. A. 2003, AJ, 129, 2102
 Wyithe, J. S. B., & Loeb, A., ApJ submitted, astro-ph/0508604